Asymmetric electron and hole transport in a high-mobility n-type conjugated polymer

Wetzelaer, Gert-Jan A. H.; Kuik, Martijn; Olivier, Yoann; Lemaur, Vincent; Cornil, Jerome; Fabiano, Simone; Loi, Maria Antonietta; Blom, Paul W. M.; Cornil, Jérôme

Published in:
Physical Review. B: Condensed Matter and Materials Physics

DOI:
10.1103/PhysRevB.86.165203

Publication date:
2012

PHYSICAL REVIEW B **86**, 165203 (2012)

Asymmetric electron and hole transport in a high-mobility *n*-type conjugated polymer

Gert-Jan A. H. Wetzelaer,[1,2] Martijn Kuik,[1] Yoann Olivier,[3] Vincent Lemaur,[3] Jérôme Cornil,[3] Simone Fabiano,[1] Maria Antonietta Loi,[1] and Paul W. M. Blom[1,4]

[1]*Molecular Electronics, Zernike Institute for Advanced Materials, University of Groningen, Nijenborgh 4, 9747 AG Groningen, The Netherlands*

[2]*Dutch Polymer Institute, P.O. Box 902, 5600 AX Eindhoven, The Netherlands*

[3]*Laboratory for Chemistry of Novel Materials, University of Mons, Place du Parc 20, 7000 Mons, Belgium*

[4]*TNO/Holst Centre, High Tech Campus 31, 5605 AE Eindhoven, The Netherlands*

(Received 4 August 2012; revised manuscript received 1 October 2012; published 18 October 2012)

Electron- and hole-transport properties of the *n*-type copolymer poly{[*N*,*N*′-bis(2-octyldodecyl)-naphthalene-1,4,5,8-bis(dicarboximide)-2,6-diyl]-*alt*-5,5′-(2,2′-dithiophene)} [P(NDI2OD-T2), PolyeraActivInk^{TM} N2200] are investigated. Electron- and hole-only devices with Ohmic contacts are demonstrated, exhibiting trap-free space-charge-limited currents for both types of charge carriers. While hole and electron mobilities are frequently equal in organic semiconductors, room-temperature mobilities of 5×10^{-8} m^2/V s for electrons and 3.4×10^{-10} m^2/V s for holes are determined, both showing universal Arrhenius temperature scaling. The origin of the large difference between electron and hole mobility is explained by quantum-chemical calculations, which reveal that the internal reorganization energy for electrons is smaller than for holes, while the transfer integral is larger. As a result, electron transport is intrinsically superior to hole transport under the same injection and extraction conditions.

DOI: 10.1103/PhysRevB.86.165203 PACS number(s): 72.80.Le, 71.38.−k, 85.30.Fg, 72.20.Jv

I. INTRODUCTION

Organic semiconductors are promising candidates for replacing conventional inorganic semiconductors in electronic devices such as solar cells, light-emitting diodes, and field-effect transistors.[1–4] A common feature of most organic semiconductors is that electron and hole transport is highly unbalanced in electronic devices.[5,6] As a consequence, materials are usually labeled either *n* or *p* type. In inorganic semiconductors, *n*- or *p*-type behavior is typically the consequence of an increased density of charge carriers induced by the addition of impurities that act as dopants. In contrast, most organic semiconductors can be considered intrinsic and unbalanced transport arises from the presence of extrinsic charge traps hindering the transport of one type of charge carrier.[5–7] Due to this charge trapping, organic electronic devices frequently exhibit only unipolar behavior. However, by using field-effect transistors with appropriate dielectrics, the charge-carrier densities are sufficiently large to fill all the traps.[8] By eliminating traps by doping in space-charge-limited diodes,[9] it has been shown that the charge-carrier mobility for electrons and holes is about equal for a number of organic semiconductors. This implies that the electron- and hole-transport properties in organic semiconductors are intrinsically similar.

Conjugated polymers form a particularly interesting class of organic semiconductors due to their potential for solution-based processing, enabling the possibility for low-cost, high-throughput, flexible, large-area, lightweight printed electronics. For most conjugated polymers, hole transport appears to be superior to electron transport in electronic devices. In diodes fabricated from these conjugated polymers, hole currents show trap-free, space-charge-limited behavior, whereas electron transport is largely reduced by the presence of charge trapping.[5,7] These electron traps are usually associated with oxygen- or water-induced impurities.[9–14] It has been shown by De Leeuw *et al.*[15] that organic materials show *n*-type stability against water when their electron affinity is greater than ∼4 eV. Therefore, for the development of stable electron-transporting materials, high electron affinities are required. This leads to a twofold advantage for electronic devices: (i) the elimination of oxygen- or water-induced charge traps and (ii) reduction of the electron injection barrier from nonreactive metal electrodes.

Recently, a high-mobility electron-transporting polymer, poly{[*N*,*N*′-bis(2-octyldodecyl)-naphthalene-1,4,5,8-bis(dicarboximide)-2,6-diyl]-*alt*-5,5′-(2,2′-dithiophene)} [P(NDI2OD-T2), PolyeraActivInk^{TM} N2200], was developed, consisting of a naphthalene diimide core (NDI), connected with a bithiophene unit (T-T), as displayed in Fig. 1.[16] Apart from its high electron mobility, this polymer is particularly interesting because of its energy levels: The lowest unoccupied molecular orbital (LUMO) is located at ~ -4 eV, while the highest occupied molecular orbital (HOMO) is situated at an energy of ~ -5.6 eV.[17] This implies that the LUMO is low enough for stable, trap-free electron transport, while the HOMO is sufficiently shallow for efficient hole injection. As a result, N2200 is an ideal compound for a detailed investigation of both electron and hole transport in a single material. In this paper, we demonstrate trap-free electron- and hole- transport measurements in N2200, enabling direct evaluation of the charge-carrier mobilities. The electron mobility is observed to be more than two orders of magnitude higher than the hole mobility, which is supported by a quantum-chemical study.

II. EXPERIMENT

The polymer N2200 was obtained from Polyera Corporation and used as received. Sandwich-type devices were fabricated on top of thoroughly cleaned glass substrates and glass substrates were prepatterned with indium tin oxide (ITO). Electron-only devices were fabricated by evaporating

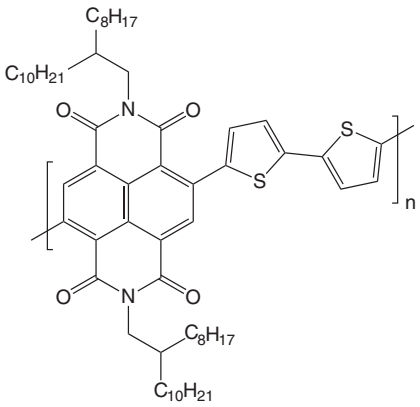

FIG. 1. Chemical structure of N2200.

an Al crossbar structure on cleaned glass substrates as a noninjecting bottom contact. Subsequently, a layer of N2200 was spin cast from toluene solution under N_2 atmosphere. The devices were finished by thermal evaporation of a Cs_2CO_3(1 nm)/Al(100 nm) cathode in vacuum (1×10^{-6} mbar). For the hole-only devices, cleaned glass/ITO substrates were spin coated with a layer of poly(3,4-ethylenedioxythiophene):poly(styrenesulfonic acid) (PEDOT:PSS) with a thickness of 60 nm, which was used to block the injection of electrons. Next, the N2200 layer was applied by spin coating and an MoO_3(10 nm)/Al(100 nm) anode was evaporated subsequently. Electron- and hole-only devices were not exposed to air from the moment of depositing the N2200 layer until finishing the electrical measurements. Electrical measurements on the sandwich-type devices were conducted under a controlled N_2 atmosphere, using a computer-controlled Keithley 2400 sourcemeter.

Thin-film transistors in staggered top-gate geometry were fabricated by spin coating the semiconductor solution (10 mg mL^{-1}) on glass substrates with bottom Au contacts (channel dimensions of $W = 500$ μm and $L = 50$ μm). After spinning the active layer, samples were annealed in vacuum oven at 120 °C overnight. The poly(methyl methacrylate) (PMMA) top-gate dielectric was spin coated from a 80 mg mL^{-1} ethyl acetate solution at 1000 rpm (700–800 nm, $k = 3.6$) and annealed at 120 °C for 2 h. Deposition of the top Al gate electrode completed the staggered thin-film transistors. The current-voltage characteristics were measured in air at room temperature using a Keithley 4200-SCS semiconductor parameter analyzer and mobility was evaluated in the saturation regime.

III. RESULTS AND DISCUSSION

A. Electron transport

Measurements on the bulk electron transport of N2200 have been carried out recently by Steyrleuthner *et al.*[18] In their report, a high electron mobility of 5×10^{-7} m^2/V s at room temperature was extracted from time-of-flight (TOF) measurements. Interestingly, the accompanying dc current measurements on electron-only diodes yielded considerably smaller values for the electron mobility. The apparent mobility was observed to increase with layer thickness, leading to the conclusion that the device current was injection limited, rather than limited by the bulk of the material. This is particularly surprising since the Fermi levels of the used cathode materials (e.g., barium) are expected to easily align with the low LUMO of N2200 to ensure Ohmic electron injection. Nevertheless, a convincing electric-field scaling of the current was presented for a wide range of layer thicknesses, which is characteristic of an injection-limited current. However, the origin of this behavior remained unclear. To enable a reliable investigation of the electron transport by means of single-carrier diodes, the problem of inefficient electron injection has to be overcome, so that true bulk-limited currents can be measured.

For the charge-transport measurements carried out in this study, single-carrier diodes were prepared. Electron-only diodes were fabricated, comprising a layer of N2200 sandwiched between an aluminum bottom and top electrode. To enhance electron injection from the top electrode, a Cs_2CO_3 layer (1 nm) was thermally evaporated on top of the polymer layer, prior to evaporation of the Al (100 nm) top electrode. Cs_2CO_3 has been frequently utilized as an efficient electron injection layer in polymer diodes.[19–24] Cesium carbonate decomposes into cesium oxides upon thermal evaporation and the resultant film is considered to be a heavily doped n-type semiconductor with an intrinsically low work function.[24] Therefore, thermally evaporated cesium carbonate exhibits good electron-injecting properties.

In case of an Ohmic electron contact, electron currents are expected to exhibit space-charge-limited conduction in case of trap-free transport. Space-charge-limited currents are widely observed in conjugated polymers[5] and are characterized by a quadratic voltage dependence and a third-power thickness dependence, according to[25]

$$J = \frac{9}{8}\varepsilon_0\varepsilon_r\mu\frac{V^2}{L^3}, \tag{1}$$

where J is the current density, ε the dielectric constant, μ the charge-carrier mobility, V the applied voltage, and L the layer thickness.

The measured electron-only currents are plotted as a function of the applied voltage (corrected for the built-in voltage V_{bi}) for a range of layer thicknesses in Fig. 2. In contrast to the measurements of Steyrleuthner *et al.*,[18] the currents do not scale with the electric field, but show an L^3 thickness dependence. In addition, the currents exhibit a quadratic dependence on voltage in the low-field regime and can therefore be described by Eq. (1). The extracted value for the zero-field mobility is 5×10^{-8} m^2/V s for all layer thicknesses. The excellent agreement with space-charge-limited conduction is a strong indication that the measured electron currents are bulk limited when using a Cs_2CO_3/Al cathode. The obtained mobility is, however, an order of magnitude lower than the previously reported value from TOF measurements. This discrepancy may well be attributed to variations in different polymer batches or by morphology variations due to different fabrication methods.[26] It should also be noted that the TOF transient in Ref. 18 shows clearly dispersive transport, implying that the transient mobility is an upper limit rather than an average value.

As can be observed in Fig. 2, the experimental data can be well described by Eq. (1) in the low-field regime. However,

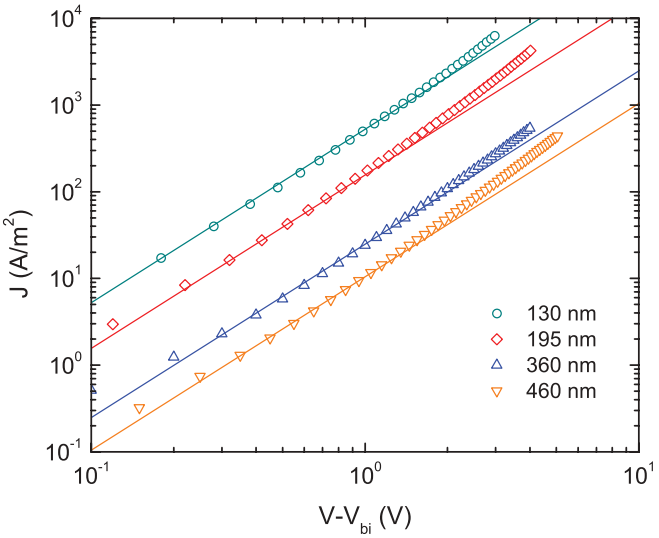

FIG. 2. (Color online) Experimental J-V characteristics (symbols) of N2200 electron-only diodes for a range of layer thicknesses. The solid lines are fits to the experimental data, calculated by Eq. (1).

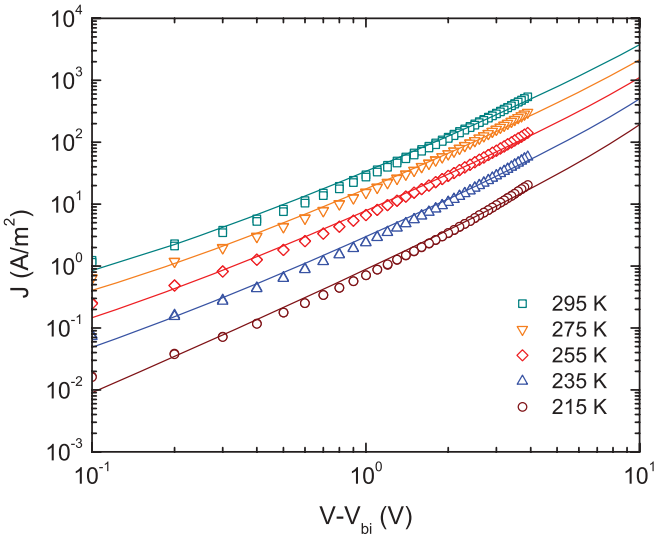

FIG. 3. (Color online) Temperature-dependent J-V characteristics (symbols) of an N2200 electron-only diode with a layer thickness of 360 nm and the corresponding calculations (solid lines) from a drift-diffusion model.

at higher applied fields, the current starts to deviate from the quadratic voltage dependence. This enhancement of the space-charge-limited current arises from the charge-density and electric-field dependence of the mobility.[27] The description of a charge-carrier density-dependent mobility can be obtained from a numerical solution of the master equation for hopping transport in a disordered energy system with a Gaussian density of states (DOS) distribution. The field, density, and temperature dependence of the mobility then follows from the choice of the width of the DOS distribution σ and the intersite spacing a, as described by[28]

$$\mu_n(T,n,E) \approx \mu_n(T,n) f(T,E), \tag{2}$$

$$\mu_n(T,n) = \mu_0(T) \exp\left[\tfrac{1}{2}(\hat{\sigma}^2 - \hat{\sigma})(2na^3)^{\delta}\right], \tag{3}$$

$$\delta \equiv 2\frac{\ln(\hat{\sigma}^2 - \hat{\sigma}) - \ln(\ln 4)}{\hat{\sigma}^2}, \tag{4}$$

$$f(T,E) = \exp\left\{0.44(\hat{\sigma}^{3/2} - 2.2)\left[\sqrt{1 + 0.8\left(\frac{Eea}{\sigma}\right)^2} - 1\right]\right\}, \tag{5}$$

where $\mu_0(T)$ is the mobility in the limit of zero charge-carrier density and electric field, T the temperature, E the electric field, and n the charge-carrier density. The normalized Gaussian variance is defined as $\hat{\sigma} \equiv \sigma / k_B T$, with k_B the Boltzmann constant. To provide a full description of the measured device currents, this field, density, and temperature dependence of the mobility needs to be taken into account. Therefore, the experimental data were fitted using a numerical drift-diffusion model.[29]

Figure 3 shows the temperature-dependent J-V characteristics of an electron-only device with a thickness of 360 nm. The fits are obtained from the numerical drift-diffusion model using $\sigma = 0.085$ eV and $a = 2.2$ nm. This set of parameters was found to excellently describe the temperature-dependent characteristics for the entire range of layer thicknesses. The accurate agreement for the field, density, and temperature dependence using a single set of parameters confirms the observation of bulk-limited electron currents. The width of the DOS distribution is considerably smaller than usually obtained for conjugated polymers, indicating a low degree of energetic disorder of the LUMO. The observation of weak disorder is in agreement with the high values obtained for the bulk electron mobility, together with its small temperature activation.

The good agreement of the current-voltage characteristics with Eq. (1) in the low-field and density regime and the accurate description of the data with the numerical simulations show that electron transport is essentially trap free. However, when the charge concentration exceeds the trap density, the effect of traps becomes invisible in the current-voltage characteristics. This puts an upper limit on the trap density of about 5×10^{-21} m^{-3}.[30] Although we cannot exclude the presence of a small shallow-trap concentration, it is clear that electron transport does not exhibit the distinct features of the usually observed trap-limited electron conduction in conjugated polymers.[14]

B. Hole transport

Up to now, just a few conjugated polymers have exhibited both p- and n-type conduction.[31] In the literature,[16–18,26] N2200 has been essentially used as an electron transporting material and no hole conduction has been evidenced so far. As we have shown in the previous section, it is crucial to carefully choose the nature of the electrode in order to provide trap-free electron transport characterized in Fig. 2 by the quadratic voltage and third-power thickness dependence of the device current. It would be thus interesting to investigate now whether hole transport can be achieved, if it is also trap free in N2200, and how it compares to the obtained characteristics for electron transport.

To investigate the hole transport, hole-only diodes were prepared. Because of the relatively deep HOMO of N2200

(~ -5.6 eV), a barrier for hole injection from common anodes such as gold [work function of 4.8 eV (Ref. 32)] or poly(3,4-ethylenedioxythiophene):poly(styrenesulfonic acid) (PEDOT:PSS), which has a work function of 5.0–5.2 eV,[30,33,34] is expected. Recently, it was demonstrated that Ohmic charge injection can be achieved by using an MoO_3 hole-injection layer for conjugated polymers comprising a HOMO as deep as -5.8 to -6.0 eV.[35] Thermally evaporated molybdenum trioxide is an n-type semiconductor with a work function as high as 6.86 eV,[36] resulting in good hole injection even for polymers with a deep HOMO. Therefore, hole-only diodes were fabricated with an MoO_3(10 nm)/Al(100 nm) top electrode, using PEDOT:PSS-covered indium tin oxide as the bottom electrode. As expected, hole injection is considerably more efficient from MoO_3 as compared to injection from the PEDOT:PSS counter electrode. For MoO_3 as Ohmic hole-injection contact, the hole currents exhibit a quadratic dependence on voltage and an L^3 thickness dependence, as displayed in Fig. 4. This is indicative of trap-free space-charge-limited hole transport, as also observed previously for electron transport. By using Eq. (1), a zero-field hole mobility of 3.4×10^{-10} m^2/V s was determined.

As was done for the electron transport, numerical drift-diffusion simulations were carried out to fully describe the field, density, and temperature dependence of the hole transport. Figure 5 depicts the temperature-dependent J-V characteristics of a hole-only device with a thickness of 140 nm. For all investigated layer thicknesses, the temperature-dependent hole current could be accurately described with a single set of parameters. The extracted values for the DOS variance and the intersite spacing were $\sigma = 0.13$ eV and $a = 1.3$ nm, respectively. Apparently, hole transport exhibits a significantly stronger disorder than electron transport. This is also reflected in the lower hole mobility, as compared to the electron mobility, as well as in the larger temperature activation for hole transport.

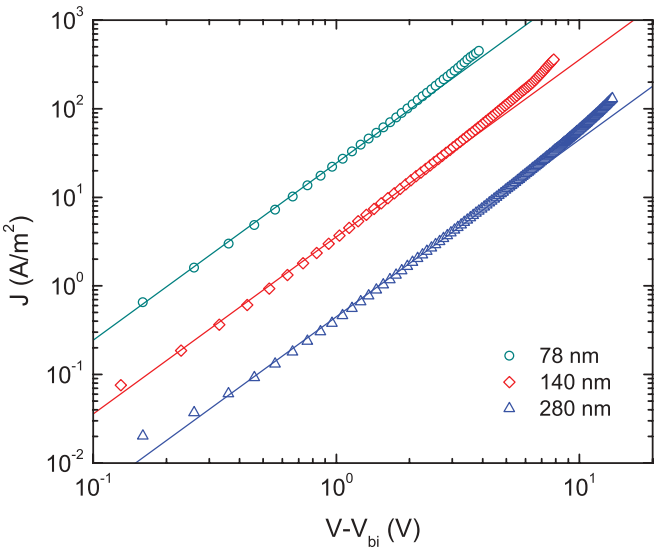

FIG. 4. (Color online) Experimental J-V characteristics (symbols) of N2200 hole-only diodes for a range of layer thicknesses. The solid lines are fits to the experimental data, calculated by Eq. (1).

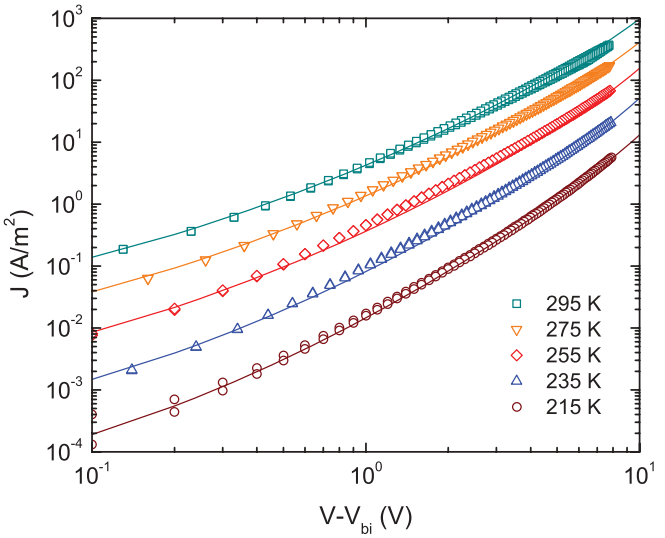

FIG. 5. (Color online) Temperature-dependent J-V characteristics (symbols) of an N2200 hole-only diode with a layer thickness of 140 nm and the corresponding calculations (solid lines) from a drift-diffusion model.

C. Temperature activation of electron and hole transport

The simultaneous observation of trap-free electron and hole transport in a conjugated polymer diode is highly exceptional. As shown in the previous sections, it conveniently enables determination of the electron and hole mobility from the space-charge-limited diode current. Interestingly, for this polymer, the electron and hole mobility differ by more than two orders of magnitude. Furthermore, the disorder parameter deduced from drift-diffusion simulations is considerably larger for holes than for electrons. It is well known that stronger disorder gives rise to a larger temperature activation for charge transport.[37] Recently, it was demonstrated that there exists a universal relation between the charge-carrier mobility and its temperature activation in organic diodes.[38] It would be interesting to see if this universal relation also applies for trap-free electron and hole transport in a single material, especially when the electron and hole mobilities are substantially different, as is the case in N2200. Figure 6 shows the extracted electron and hole mobilities as a function of temperature. As is usually observed for organic semiconductor diodes, the charge-carrier mobility exhibits an Arrhenius temperature dependence, according to

$$\mu(T) = \mu_\infty \exp\left(-\frac{\Delta}{k_B T}\right), \tag{6}$$

with μ_∞ the charge-carrier mobility in the limit of zero field and infinite temperature and Δ the activation energy. Remarkably, both electron and hole mobilities extrapolate to the previously reported universal value for the mobility of 30 cm^2/V s at infinite temperature.[38] So both electron and hole mobilities, although they differ by more than two orders of magnitude, individually follow the universal scaling behavior as observed for organic semiconductors. Such behavior is usually experimentally elusive, since in most cases charge trapping effects obscure the transport properties of one of the two types of charge carriers. Moreover, charge-carrier

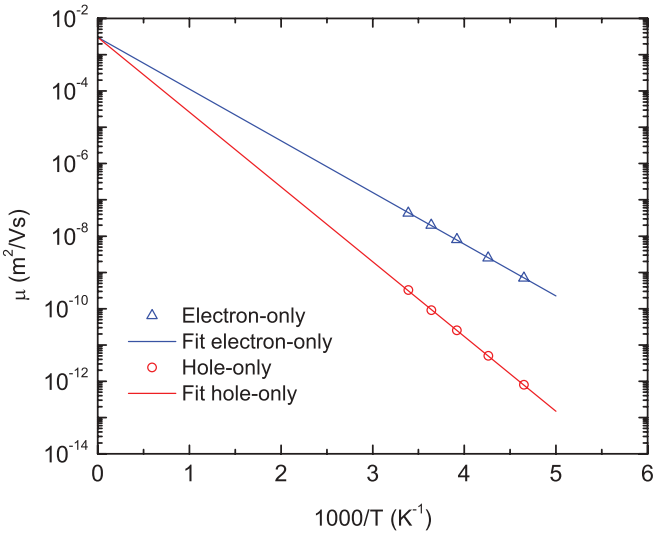

FIG. 6. (Color online) Measured low-field mobilities for N2200-based single-carrier diodes. The solid lines are the best fits to the experimental data, using the Arrhenius temperature dependence according to Eq. (6).

mobilities in conjugated polymers are frequently similar for electrons and holes and hence similar temperature activation has been observed.[9] In N2200, however, the electron mobility is much larger than the hole mobility, which appears to be also reflected in its smaller temperature activation. The activation energy for the electron mobility was determined to be 0.28 eV, while the hole mobility was temperature activated with an activation energy of 0.41 eV. Such a difference in temperature activation is in line with the previously determined values for the width of the DOS distribution.

D. Thin-film transistors

Ambipolar transport characteristics were also observed in transistors with poly(methyl methacrylate) (PMMA) as the gate dielectric. Typical transfer characteristics are presented in Fig. 7, demonstrating operation in both electron- [Fig. 7(a)] and hole-enhancement [Fig. 7(b)] mode. An asymmetric hole and electron mobility of respectively 3.3×10^{-8} and 4.0×10^{-6} $m^2/V\,s$ was derived in the saturation regime from high gate voltage regions (for holes $V_g = -90$ V and electrons $V_g = 60$ V). These mobilities are typically two orders of magnitude higher than the values measured in the diodes, but exhibit a similar asymmetry. The reason that the field-effect transistor (FET) mobilities are higher than the diode mobilities can, at least in part, be due to the enhanced carrier densities in FETs,[27] typically amounting to 10^{24}–10^{25} m^{-3}. In addition, charge transport in FETs occurs horizontally at the polymer/dielectric interface, which can have different properties than vertical bulk transport in a diode configuration, for instance, due to mobility anisotropy. Although the mismatch in energy levels between the gold work function and the N2200 HOMO/LUMO levels results in an injection barrier φ_B of ∼0.8 eV for both electrons and holes, Fig. 7(b) shows that a large negative voltage is needed to detect the hole current, indicating the presence of a larger injection barrier for holes. In this respect, the threshold voltage, extracted from the transfer characteristic in the saturation regime, is ∼14 V for electrons and ∼ − 67 V for holes.

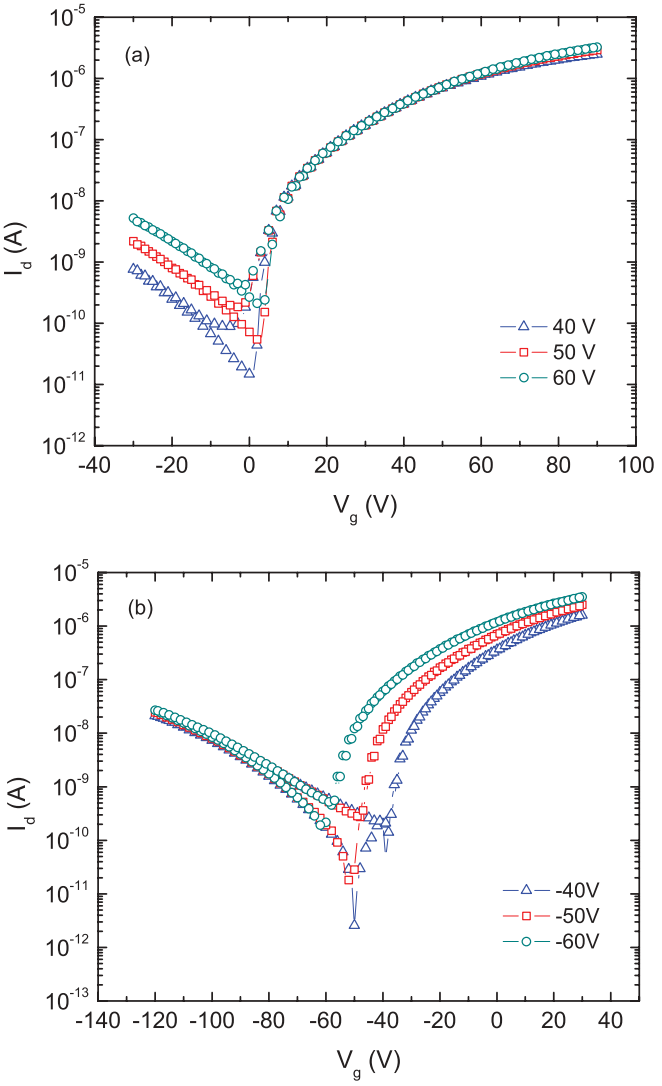

FIG. 7. (Color online) Transfer characteristics of a spin-coated N2200 thin-film transistor for both *n*-channel (a) and *p*-channel (b) operation.

E. Quantum-chemical calculations

Usually, electron and hole mobilities have similar values in conjugated homopolymers.[8,9] From the measurements on electron- and hole-only devices, it appears that the electron mobility is considerably higher than the hole mobility in the bulk of N2200. One of the reasons can certainly be found in the larger energetic disorder for hole transport as compared to electron transport. In addition, positional disorder as well as polaronic effects should also be considered in order to give an accurate picture of charge transport in this polymer.[39] These contributions are often difficult to assess experimentally since a reasonable description of the supramolecular morphology is required. To address this issue, quantum-chemical calculations have been carried out on model systems.

The two parameters characterizing charge transport in the hopping regime are the reorganization energy λ and the transfer

integral J, which appear explicitly in the expression of the Marcus charge hopping rate as[40]

$$k = \frac{2\pi}{\hbar} J^2 \frac{1}{\sqrt{4\pi\lambda k_B T}} \exp\left(-\frac{\lambda}{4k_B T}\right), \tag{7}$$

with $\hbar$ the reduced Planck constant. The reorganization energy λ is the sum of the internal reorganization energy λ_i, which accounts for the reorganization of the molecular geometry upon oxidation or reduction, and the external reorganization energy λ_S, which accounts for the change in the nuclear polarization of the molecules in the surrounding of the charge during the charge-transfer process. From calculations on single crystals,[41–43] it appears that the main contribution to the total reorganization energy is due to the geometric reorganization of the molecules involved in the charge transfer since the internal contribution is on the order of hundreds of meV while the external part is less than few tenths of meV.

In order to investigate the intrinsic charge-transport properties of N2200, we have considered oligomers of N2200 going from 1 to 3 monomer units and have calculated their electronic structures and reorganization energies. The optimization of the geometry has been achieved at the density functional theory (DFT) level with the Becke three-parameter Lee-Yang-Parr (B3LYP) hybrid functional and the 6-31G** basis set. This methodology has been extensively used and has shown good agreement with experimental estimates of the reorganization energy.[44]

1. Torsion potential calculations

Recently, x-ray scattering experiments[45] performed on N2200 thin films have revealed unconventional face-on stacking and a high degree of in-plane crystallinity. It has been evidenced that the N2200 polymer chains are found to be almost positioned with the NDI units in a cofacial configuration. However, the planarity of the molecular geometry of this polymer was not discussed. In the model compounds considered in our calculations, we have identified two different torsional degrees of freedom, namely, (i) the torsion between the naphthalene-di-imide (NDI) unit and the first thiophene (T) unit and (ii) the torsion between the thiophene rings.

The energetic profile corresponding to the torsion between the NDI unit and the closer thiophene ring within the N2200 monomer exhibits two minima very close in energy (see Fig. 8, $\Delta E = 0.2$ kcal/mol) around 40° and 130° corresponding to the conformations where the hydrogen atoms and the sulfur atom of the first thiophene ring are pointing to the adjacent oxygen atom of the NDI unit, respectively. From these minima, two very large energetic barriers ($\Delta E = 2.5$ kcal/mol) have been estimated at 0° and 180° while one relatively high ($\Delta E =$ 1.3 kcal/mol, i.e., much larger than $k_B T$) has been calculated at 90°. Therefore, our results suggest that two conformers should coexist but that the conversion from one conformer to the other is unlikely in the solid state for steric reasons.

In the following, the conformers with the torsion angles at 40° and 130° are renamed NDI-T-$T_{40°}$ and NDI-T-$T_{130°}$, respectively. Regarding the thiophene-thiophene torsion potential within the N2200 monomer, as expected, the *trans*-conformation is more stable than the *cis*-conformation with a substantially higher barrier (∼4 kcal/mol) compared to NDI-T, making a flipping of the thiophene ring at room temperature very unlikely, especially in the solid state.

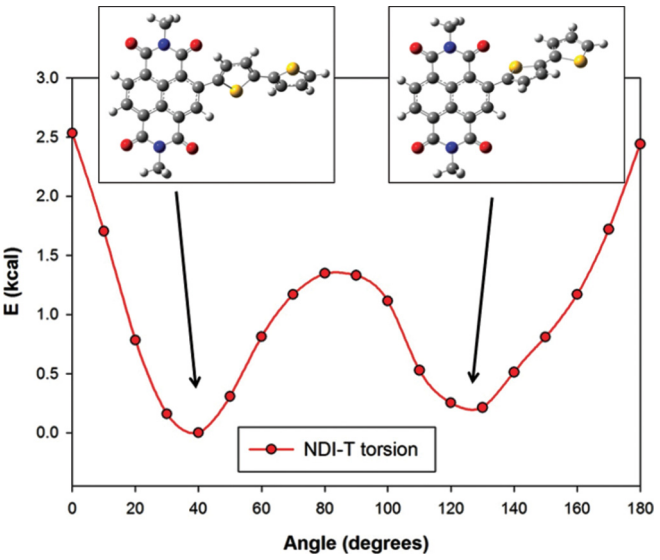

FIG. 8. (Color online) DFT-calculated (B3LYP/6-31G**) torsion potential between the NDI unit and the first thiophene ring within the N2200 monomer. Representation of the two different conformers.

2. Electronic structure and reorganization energy calculations

For the calculations of the electronic structure and reorganization energy, we have considered oligomers of increasing size. Interestingly, the HOMO (LUMO) orbitals are strongly localized on the electron-poor thiophene (electron-rich NDI) units, showing the strong donor and acceptor character difference between the NDI and bithiophene fragments (Fig. 9).

To estimate the reorganization energy, we have considered the initial conformation of the different oligomers corresponding to the energy minima obtained from the torsion potentials, namely, either 40° or 130° for the NDI-T torsion and 165° (*trans*-conformation) for the thiophene-thiophene torsion angle.

For the monomers, the optimization of the different charged states has revealed quite different evolutions in the torsion angle, as shown in Table I. The positive polaron exhibits a large difference in torsion angle and tends to planarize the bithiophene unit while the negatively charged state is only slightly modified. The *trans*-conformation between the thiophene rings is kept.

The calculated reorganization energies (Table II) for the positive polarons are larger as compared to the negative polarons for each of the systems considered. Two major reasons contribute to this difference: (i) the number of atoms on which the HOMO and LUMO orbitals are delocalized and

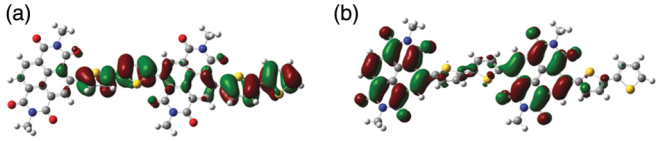

FIG. 9. (Color online) (a) HOMO and (b) LUMO orbitals for the N2200 dimer in its neutral state.

TABLE I. DFT-calculated (B3LYP/6-31G**) torsion angles between the different units in the two different conformers of the N2200 monomer in the neutral and charged states.

		Neutral	Positive	Negative
NDI-T-T_{40}	NDI-T torsion (deg)	39	47	40
	T-T torsion (deg)	160	178	163
NDI-T-T_{130}	NDI-T torsion (deg)	125	47	120
	T-T torsion (deg)	–157	–177	–160

(ii) the amplitude of the change in the torsion angle between the neutral and charged states. Indeed, if more atoms are involved in the delocalization of an orbital, smaller bond length changes are expected upon oxidation or reduction, which hence reduces the internal reorganization energy while larger torsion angle differences between the neutral and charged compounds will lead to an increase in the internal reorganization energy. The difference in reorganization energy cannot be obviously explained on the basis of the changes in bond lengths since they appear to be quite similar for both polaronic states (deviations of ∼0.03 Å, in agreement with Refs. 46 and 47). As illustrated for the monomer (Table I) and confirmed for longer oligomers, the torsion angle difference between the neutral state and the polaronic state is larger for positive than for negative polarons. These variations in torsion angles between both charged states are responsible for the difference in reorganization energy. Moreover, we have noticed that the internal reorganization energies associated with the negative polarons are similar for both conformers while the internal reorganization energies associated with the positive polarons are much smaller for NDI-T-T_{40} since going from the neutral state to the positive polaron of NDI-T-T_{130} involves larger changes in the torsion angles.

3. *Transfer integral calculations*

The transfer integral J (i.e., electronic coupling) has often been estimated as half of the splitting of the HOMO (LUMO) levels in a neutral dimer for hole (electron) transport.[48] However, this approach is often biased by polarization effects, which in noncentrosymmetric structures create an energy offset of the electronic levels that does not contribute to the transfer efficiency.[49,50] Reliable values of J are thus obtained from the estimation of the direct interaction between the orbitals of the molecules involved in the charge transfer ($\psi_{i,j} \equiv$ HOMOs or LUMOs) $\psi_i|H|\psi_j$, with this matrix element calculated in an orthogonal $\{\psi_i\}$ basis set.[49,51]

TABLE II. Hole (λ_i^h) and electron (λ_i^e) internal reorganization energies calculated for both conformers of increasing length.

		$n=1$	$n=2$	$n=3$
$(\text{NDI-T-T}_{40})_n$	λ_i^h (eV)	0.32	0.24	0.16
	λ_i^e (eV)	0.28	0.16	0.12
$(\text{NDI-T-T}_{130})_n$	λ_i^h (eV)	0.46	0.38	0.27
	λ_i^e (eV)	0.29	0.19	0.14

Since the transfer integral is highly sensitive to the relative orientation of the molecules,[39] it is of the utmost importance to have a reasonable model for the packing of the polymer chains involved in the charge transport. Recently, a model of the packing of the NDI-T-T polymer chains has been elaborated from x-ray scattering measurements,[45] suggesting that the chains are superimposed. Starting from this model, displacements along the polymer axis lead to energetically unfavorable packings. Therefore, the polymer chains are clicked due to the NDI-T torsion angle limiting displacements along the polymer chain. Therefore, the only remaining degree of freedom is the displacement of the oligomer chains along the axis joining the two nitrogen atoms of the NDI unit (see Fig. 10). Transfer integral calculations have been performed both for hole and electron transport by looking at the influence of a displacement along this direction. In this study, a molecular complex made of two oligomers containing two monomer units has been considered for each conformation.

The evolution of the transfer integrals as a function of the displacement along the axis joining the two nitrogen atoms of the NDI unit is displayed in Fig. 11. The behavior of the transfer integral for electrons is quite similar for both conformers, which is not surprising since their LUMO orbitals are quite similar (mainly localized on the NDI unit). On the other hand, in our model system, the transfer integrals are smaller for holes than for electrons for most of the dimers considered. This originates from the different aspect ratios of the different units of the N2200 polymer. Indeed, due to the larger size of the NDI unit compared to the thiophene, the spatial overlap decreases more quickly for thiophenes on adjacent chains than for NDI units when polymer chains are translated. Finally, electron transport appeared to be less sensitive to displacements than hole transport, in agreement with a recent theoretical study using a similar methodology on different N2200 structures.[46,47]

The larger spread in the transfer integral for holes as a function of displacements can be interpreted as larger

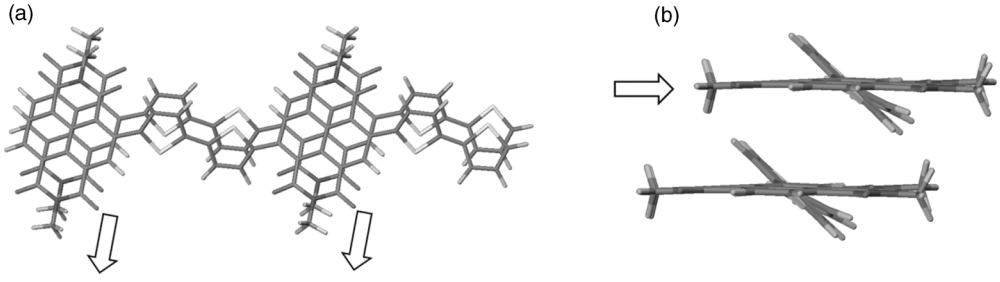

FIG. 10. (a) Top and (b) side views of the NDI-T polymer chains displacement along the axis joining the two nitrogen atoms.

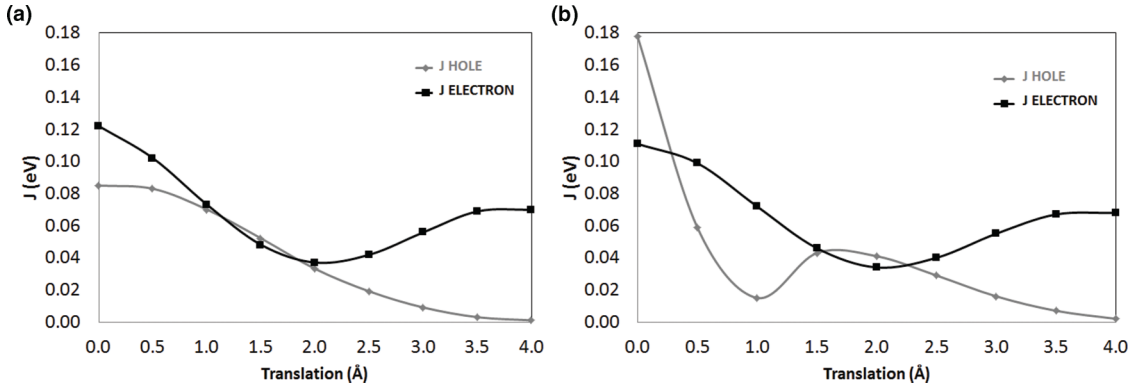

FIG. 11. Calculated transfer integrals [J_{HOMO} (gray diamonds) and J_{LUMO} (black squares)] obtained by displacing along the axis joining the nitrogen atoms of the NDI units one oligomer within a dimer characterized by an intermolecular distance of 4 Å between the NDI units for (a) the 40° and (b) 130° torsion angle conformers.

positional disorder. In terms of the Gaussian disorder model, this would be reflected in a larger width of the Gaussian DOS distribution of the HOMO as compared to the LUMO. This is in agreement with the larger disorder parameter σ for holes that was extracted from modeling the experimental current-voltage characteristics of hole-only diodes with the extended Gaussian disorder model[28] as done in previous sections. In addition, the larger reorganization energy, in combination with larger positional disorder, will lead to a higher temperature activation for hole transport, which has been observed experimentally.

In the end, looking back at the expression for the Marcus charge-transfer rate [Eq. (7)], it appears that the hopping rate is maximized for a large transfer integral and a small reorganization energy. As a result, electron transport has to be intrinsically better than hole transport under the same charge injection and extraction conditions.

IV. CONCLUSIONS

In conclusion, we found intrinsically asymmetric bulk electron and hole transport in the *n*-type polymer N2200. Electron- and hole-only devices of N2200 were fabricated and Ohmic electron and hole contacts were demonstrated. Remarkably, both electron and hole currents showed trap-free space-charge-limited behavior. As a result of the unusual absence of extrinsic charge traps for both types of charge carriers, intrinsic charge-transport properties could be evaluated. Room-temperature mobilities of 5×10^{-8} $\mathrm{m^2/V\,s}$ for electrons and 3.4×10^{-10} $\mathrm{m^2/V\,s}$ for holes were determined for the bulk transport through the polymer. Furthermore, electron and hole transport was observed to follow universal Arrhenius temperature scaling with an activation energy of 0.28 and 0.41 eV, respectively. The observation of such temperature scaling for both electrons and holes in a single organic semiconductor is exceptional, since the transport of one of the two carriers is usually obscured by trapping effects. The large difference between electron and hole transport was rationalized by quantum-chemical calculations, which revealed that the internal reorganization energy is smaller and the transfer integral is larger for electrons as compared to holes. As a consequence, electron transport is intrinsically better than hole transport, when the same injection and extraction conditions are considered.

ACKNOWLEDGMENTS

The authors acknowledge the technical assistance of Jan Harkema. The work of G.A.H.W. is supported by the Dutch Polymer Institute (DPI), Project No. 678. The work in Mons is supported by the European ONE-P (NMP3-LA-2008-212311) project, by the European Commission/Région Wallonne (FEDER–Smartfilm RF project), the OPTI2MAT excellence program (Région Wallonne), as well as by the Belgian National Fund for Scientific Research (FNRS). Y.O. and J.C. are supported by FNRS research fellowships. The calculations were performed on the Interuniversity Scientific Calculation Facility (ISCF) installed at the Facultés Universitaires Notre-Dame de la Paix (FUNDP, Namur, Belgium), for which we gratefully acknowledge financial support from the FRS-FRFC (Convention No. 2.4.617.07.F), and FUNDP.

[1]C. W. Tang and S. A. VanSlyke, Appl. Phys. Lett. **51**, 913 (1987).
[2]J. H. Burroughes, D. D. C. Bradley, A. R. Brown, R. N. Marks, K. Mackay, R. H. Friend, P. L. Burns, and A. B. Holmes, Nature (London) **347**, 539 (1990).
[3]G. Yu, J. Gao, J. C. Hummelen, F. Wudl, and A. J. Heeger, Science **270**, 1789 (1995).
[4]H. Klauk, Chem. Soc. Rev. **39**, 2643 (2010).
[5]P. W. M. Blom, M. J. M. de Jong, and J. J. M. Vleggaar, Appl. Phys. Lett. **68**, 3308 (1996).
[6]J. Zaumseil and H. Sirringhaus, Chem. Rev. **107**, 1296 (2007).
[7]M. M. Mandoc, B. de Boer, G. Paasch, and P. W. M. Blom, Phys. Rev. B **75**, 193202 (2007).
[8]L. L. Chua, J. Zaumseil, J. F. Chang, E. C. W. Ou, P. K. H. Ho, H. Sirringhaus, and R. H. Friend, Nature (London) **434**, 194 (2005).

[9]Y. Zhang, B. de Boer, and P. W. M. Blom, Phys. Rev. B **81**, 085201 (2010).
[10]H.-E. Tseng, K.-Y. Peng, and S.-A. Chen, Appl. Phys. Lett. **82**, 4086 (2003).
[11]V. Kažukauskas, Semicond. Sci. Technol. **19**, 1373 (2004).
[12]T. D. Anthopoulos, G. C. Anyfantis, G. C. Papavassiliou, and D. M. de Leeuw, Appl. Phys. Lett. **90**, 122105 (2007).
[13]J.-M. Zhuo, L.-H. Zhao, R.-Q. Png, L.-Y. Wong, P.-J. Chia, J.-C. Tang, S. Sivaramakrishnan, M. Zhou, E. C.-W. Ou, S.-J. Chua, W.-S. Sim, L.-L. Chua, and P. K.-H. Ho, Adv. Mater. **21**, 4747 (2009).
[14]H. T. Nicolai, M. Kuik, G. A. H. Wetzelaer, B. de Boer, C. Campbell, C. Risko, J. L. Brédas, and P. W. M. Blom, Nat. Mater. **11**, 882 (2012).
[15]D. M. de Leeuw, M. M. J. Simenon, A. R. Brown, and R. E. F. Einerhand, Synth. Met. **87**, 53 (1997).
[16]Z. Chen, Y. Zheng, H. Yan, and A. Facchetti, J. Am. Chem. Soc. **131**, 8 (2009).
[17]H. Yan, Z. Chen, Y. Zheng, C. Newman, J. R. Quinn, F. Dötz, M. Kastler, and A. Facchetti, Nature (London) **457**, 679 (2009).
[18]R. Steyrleuthner, M. Schubert, F. Jaiser, J. C. Blakesley, Z. Chen, A. Facchetti, and D. Neher, Adv. Mater. **22**, 2799 (2010).
[19]T. Hasegawa, S. Miura, T. Moriyama, T. Kimura, I. Takaya, Y. Osato, and H. Mizutani, SID Int. Symp. Digest. Tech. Papers **35**, 154 (2004).
[20]J. Huang, G. Li, E. Wu, Q. Xu, and Y. Yang, Adv. Mater. **18**, 114 (2006).
[21]C. Wu, C. T. Lin, Y. Chen, M. Chen, Y. Lu, and C. C. Wu, Appl. Phys. Lett. **88**, 152104 (2006).
[22]H. J. Bolink, E. Coronado, J. Orozco, and M. Sessolo, Adv. Mater. **21**, 79 (2009).
[23]D. Kabra, L. P. Lu, M. H. Song, H. J. Snaith, and R. H. Friend, Adv. Mater. **22**, 29 (2010).
[24]J. Huang, Z. Xu, and Y. Yang, Adv. Funct. Mater. **17**, 1966 (2007).
[25]N. F. Mott and R. W. Gurney, *Electronic Processes in Ionic Crystals* (Oxford University Press, London, 1940).
[26]J. C. Blakesley, M. Schubert, R. Steyrleuthner, Z. Chen, A. Facchetti, and D. Neher, Appl. Phys. Lett. **99**, 183310 (2011).
[27]C. Tanase, E. J. Meijer, P. W. M. Blom, and D. M. de Leeuw, Phys. Rev. Lett. **91**, 216601 (2003).
[28]W. F. Pasveer, J. Cottaar, C. Tanase, R. Coehoorn, P. A. Bobbert, P. W. M. Blom, D. M. de Leeuw, and M. A. J. Michels, Phys. Rev. Lett. **94**, 206601 (2005).
[29]L. J. A. Koster, E. C. P. Smits, V. D. Mihailetchi, and P. W. M. Blom, Phys. Rev. B **72**, 085205 (2005).
[30]N. I. Craciun, J. J. Brondijk, and P. W. M. Blom, Phys. Rev. B **77**, 035206 (2008).
[31]Z. Chen, M. J. Lee, R. S. Ashraf, Y. Gu, S. Albert-Seifried, M. M. Meedom Nielsen, B. Schroeder, T. D. Anthopoulos, M. Heeney, I. McCulloch, and H. Sirringhaus, Adv. Mater. **24**, 647 (2012).
[32]K. Asadi, T. G. de Boer, P. W. M. Blom, and D. M. de Leeuw, Adv. Funct. Mater. **19**, 3173 (2009).
[33]N. Koch, A. Vollmer, and A. Elschner, Appl. Phys. Lett. **90**, 043512 (2007).
[34]T.-W. Lee, Y. Chung, O. Kwon, and J.-J. Park, Adv. Funct. Mater. **17**, 390 (2007).
[35]H. T. Nicolai, G. A. H. Wetzelaer, M. Kuik, A. J. Kronemeijer, B. de Boer, and P. W. M. Blom, Appl. Phys. Lett. **96**, 172107 (2010).
[36]M. Kröger, S. Hamwi, J. Meyer, T. Riedl, W. Kowalsky, and A. Kahn, Org. Electron. **10**, 932 (2009).
[37]H. Bässler, Phys. Status Solidi B **175**, 15 (1993).
[38]N. I. Craciun, J. Wildeman, and P. W. M. Blom, Phys. Rev. Lett. **100**, 056601 (2008).
[39]J. L. Brédas, J. P. Calbert, D. A. da Silva Filho, and J. Cornil, Proc. Natl. Acad. Sci. USA **99**, 5804 (2002).
[40]R. A. Marcus, Rev. Mod. Phys. **65**, 599 (1993).
[41]N. Martinelli, J. Idé, R. S. Sanchez-Carrera, V. Coropceanu, J. L. Brédas, L. Ducasse, F. Castet, J. Cornil, and D. Beljonne, J. Phys. Chem. C **114**, 20678 (2010).
[42]J. E. Norton and J. L. Brédas, J. Am. Chem. Soc. **130**, 12377 (2008).
[43]D. P. MacMahon and A. Troisi, J. Phys. Chem. Lett. **1**, 941 (2010).
[44]V. Coropceanu, M. Malagoli, D. A. da Silva Filho, N. E. Gruhn, T. G. Bill, and J. L. Brédas, Phys. Rev. Lett. **89**, 275503 (2002).
[45]J. Rivnay, M. F. Toney, Y. Zheng, I. V. Kauvar, Z. Chen, V. Wagner, A. Facchetti, and A. Salleo, Adv. Mater. **22**, 4359 (2010).
[46]M. Caironi, M. Bird, D. Fazzi, Z. Chen, R. Di Pietro, C. Newman, A. Facchetti, and H. Sirringhaus, Adv. Funct. Mater. **21**, 3371 (2011).
[47]D. Fazzi, M. Caironi, and C. Castiglioni, J. Am. Chem. Soc. **133**, 19056 (2011).
[48]J. L. Brédas, D. Beljonne, V. Coropceanu, and J. Cornil, Chem. Rev. **104**, 4971 (2004).
[49]E. F. Valeev, V. Coropceanu, D. A. d. Silva, S. Salman, and J. L. Brédas, J. Am. Chem. Soc. **128**, 9882 (2006).
[50]A. Van Vooren, V. Lemaur, A. Ye, D. Beljonne, and J. Cornil, Chem. Phys. Chem. **8**, 1240 (2007).
[51]L. Viani, Y. Olivier, S. Athanasopoulos, D. A. da Silva Filho, J. Hulliger, J. L. Brédas, J. Gierschner, and J. Cornil, Chem. Phys. Chem. **11**, 1062 (2010).